JOURNAL OF RESEARCH of the National Bureau of Standards—A. Physics and Chemistry
Vol. 68A, No. 6, November–December 1964

Steady-State Response of Silicon Radiation Detectors of the Diffused *p-n* Junction Type to X Rays. I: Photovoltaic Mode of Operation[1]

Karl Scharf and Julian H. Sparrow

(August 13, 1964)

A relation is derived for the photocurrent produced by x rays in silicon radiation detector cells of the *p-n* junction type, giving the dependence of the generated photocurrent on exposure rate, photon energy, and electrical and geometrical parameters of the silicon wafer. Silicon radiation detector cells operated as photovoltaic cells are found to be more sensitive to x rays than silicon solar cells previously investigated, open-circuit voltages being several hundred times larger than those measured in solar cells. The short-circuit current produced by x rays increases with increasing temperature by about 0.3 percent per °C at 25 °C cell temperature. Due to the high zero voltage junction resistance of silicon radiation detector cells, the temperature dependence of the photovoltaic output current increases with increasing load resistance at a smaller rate than that observed in silicon solar cells. The energy dependence of the short-circuit current produced by x rays, measured over a wide range of radiation qualities, is shown to be in good qualitative agreement with calculated values.

1. Introduction

In a previous investigation [1] [2] it has been reported that silicon solar cells show a quick and stable photovoltaic response to x and gamma rays and can be used for measurement of exposure rates of such radiations. Since then, several authors investigated the possibility of using silicon solar cells for x- and gamma-ray dosimetry [2,3,4].

Silicon solar cells are photovoltaic cells of the *p-n* junction type specially designed for solar energy conversion. They are made of low resistivity silicon of high impurity concentration and have a narrow depletion region and low cell resistance. In recent years, silicon *p-n* junction type cells have been developed for use in charged particle energy spectroscopy (hereafter referred to as radiation detector cells) which are made of high resistivity silicon. In such cells, the width of the depletion region and the diffusion lengths of minority carriers are much larger than in silicon solar cells. Because of their larger charge collecting volume and higher cell resistance, such cells were expected to have, compared with solar cells, a greater sensitivity for x and gamma rays and better temperature stability when operated as photovoltaic cells.

This paper reports an investigation of the steady-state response of diffused *p-n* junction type silicon radiation detector cells to x rays when operated as photovoltaic cells.[3] Quantitative measurements were made of the dependence of cell sensitivity on exposure rate, cell temperature, and quality of radiation. Furthermore, a theoretical relation was derived for the photocurrent produced by x rays, giving the dependence of the cell sensitivity on quality of radiation, and electrical and geometrical parameters of the silicon wafer.

Measurements reported here were limited to x rays of photon energies less than 250 keV, in order to avoid radiation damage possibly produced by radiations of higher photon energy.

---

[1] Supported in part by the U.S. Atomic Energy Commission.

[2] Figures in brackets indicate the literature references at the end of this paper.

[3] An investigation of the response of such cells to x rays when operated as photodiodes will be reported in a subsequent paper.

2. List of Symbols

I_g, J_g—Generated photocurrent, total (ampere) and density (ampere cm^{-2}) respectively.
$(I_g)_{Dr}$, $(J_g)_{Dr}$—Drift component of generated photocurrent, total (ampere) and density (ampere cm^{-2}), respectively.
I_{Di}, J_{Di}—Net diffusion current, total (ampere) and density (ampere cm^{-2}) respectively.
I_j, J_j—Junction leakage current, total (ampere) and density (ampere cm^{-2}) respectively.
$(I_j)_V$—Junction leakage current at forward voltage V (ampere).
I_o—Diode saturation current in reverse direction (ampere).
I_s—Short circuit current (ampere).
I—Photovoltaic output current (ampere).
V_{oc}—Open-circuit voltage (volt).
V—Photovoltage between cell terminals under closed circuit conditions (volt).
$(R_j)_V$—Static junction leakage resistance at forward voltage V (ohm).
R_L—Load resistance (ohm).
q—Electronic charge (coulomb).
kT—Thermal energy (eV).
$\Delta X/\Delta t$—Exposure rate of x rays (R/sec).
μ, μ_{en}—Linear attenuation and linear energy absorption coefficient, respectively, of silicon for x rays (cm^{-1}).
$(\mu_{en}/\rho)_{air}$—Mass energy absorption coefficient of air for x rays (cm^2 g^{-1}).
ϵ—Average electron-hole pair production energy (erg).
g—Rate of generation of electron-hole pairs due to irradiation (cm^{-3} sec^{-1}).
I_R—Radiation intensity (erg cm^{-2} sec^{-1}).
A_c, A_R—Total and irradiated cell area respectively (cm^2).
w—Width of depletion region (cm).
d_s, d_b—Widths of n-type surface layer and p-type base layer, respectively (cm).
L_p, L_n—Average diffusion lengths of minority carriers (cm).
τ_p, τ_n—Lifetimes of minority carriers (sec).
D_p, D_n—Diffusion constants of minority carriers (cm^2 sec^{-1}).
s_p, s_n—Surface recombination velocities of minority carriers (cm sec^{-1}).
p, n—Steady-state concentration of minority carriers (cm^{-3}).
p_n, n_p—Thermal equilibrium concentration of minority carriers (cm^{-3}).

3. Theoretical Considerations

3.1. Basic Equations

Under the photovoltaic mode of operation of a radiation detector cell, a photocurrent is produced in an electrical circuit connected to the cell without application of an external bias voltage. If the cell is irradiated, excess carriers are produced throughout the whole silicon wafer, but only carriers produced inside the junction or depletion region, or minority carriers produced in the bulk of the silicon reaching the junction region by diffusion, are acted upon by the junction field. Holes are driven to the p-side and electrons to the n-side of the junction, thus producing a voltage difference biasing the cell in the forward direction.

The radiation produced charge carriers separated by the junction field represent the generated photocurrent I_g, flowing in the reverse direction of the cell. Under steady-state conditions, the photovoltage V produces a back current equal to I_g. Part of it is flowing as the photovoltaic output current I through the external circuit in the reverse direction, the other part is flowing back through the cell as junction current I_j in the forward direction (fig. 14 in appendix). If the load resistance connected across the cell terminals $R_L=0$, the external or short circuit current I_s will reach its maximum value equal to I_g. Under open

circuit conditions ($R_L=\infty$), the photovoltage reaches a maximum called the open-circuit voltage V_{oc}, and the back current through the cell will be equal to I_g.

Several authors [5–9] calculated the photovoltaic output current of a p-n junction cell as a function of electrical and geometrical parameters of the cell and quality of radiation, assuming a negligible width of the junction region. Gaertner [10] and Tuzzolino et al. [11] calculated the photocurrent produced in surface barrier cells taking into account the voltage dependent width of the depletion region. All these calculations were made for the photoresponse to visible light, but similar methods of calculation can be applied to the calculation of the photocurrent produced by x rays.

In the case of x rays, secondary high-energy electrons are produced by photon-electron interactions which dissipate their energy by producing low-energy electron-hole pairs in electron-electron collisions. The number of these low-energy charge carriers contributing to the photocurrent is proportional to the *energy* of radiation absorbed and not to the *number* of absorbed photons as in the case of visible light. The average energy required to produce one electron-hole pair by electron-electron collision is approximately 3.5 eV [12], as compared with a threshold energy of approximately 1.1 eV for electron-hole pair production by light. Furthermore, a distinction must be made in the case of x rays between the attenuation coefficient and the energy absorption coefficient of the radiation, the latter determining the amount of absorbed radiation energy converted into electron energy.

For the calculation of the photocurrent produced by x rays, it was assumed that the ionization due to the reabsorption in the silicon wafer of the bremsstrahlung, fluorescence radiation and Compton photon radiation produced in the absorption process of x rays is negligibly small and need not be taken into account. Finally, *true* electronic equilibrium was assumed to exist in the silicon wafer. Under this condition, the energy per unit volume deposited by secondary electrons at a certain point in the charge collecting volume is equal to the entire energy of secondary electrons produced per unit volume by the x rays at this point.

The calculation of the photovoltaic output current produced by x rays in a p-n junction cell carried out under the above assumptions, and taking into account the ionization produced inside the depletion region, is given in the appendix. Considering the cell type investigated, it was assumed that the cell consisted of a p-type silicon base with a thin n-type layer at the irradiated surface.

The result of the calculation can be written as

$$I=I_g-I_j \tag{1}$$

where

$$I_g=\frac{86.9qA_R}{\epsilon}(\Delta X/\Delta t)\frac{(\mu_{en}/\mu)}{(\mu_{en}/\rho)_{\text{air}}}\exp(-\mu d_s)\times\left[1-\left(1-\frac{\mu L_n}{\mu^2L_n^2-1}a_n\right)\exp(-\mu w)+\frac{\mu L_p}{\mu^2L_p^2-1}a\right] \tag{2}$$

$$I_j=A_cq\left[\exp(qV/kT)-1\right]\left(\frac{p_nD_p}{L_p}b_p+\frac{n_pD_n}{L_n}b_n\right) \tag{3}$$

if I and I_g in the reverse direction are taken as positive and ϵ is given in erg and $\Delta X/\Delta t$ in R/sec.

The quantities a_p, a_n, b_p, and b_n given in the appendix (eqs (A.13)) are functions of the geometrical dimensions of the silicon wafer, and of the average diffusion lengths and surface recombination velocities of minority charge carriers. The quantities a_p and a_n are further dependent on the attenuation coefficients of silicon for x rays.

For the p-n junction type radiation detector cells considered here, it may be assumed that $d_s/L_p<<1$ and $d_b/L_n>>1$. Under these conditions and assuming small surface recombination at the base contact, approximate values of a_p and a_n can be used as given by eqs (A.20–21). Assuming further the value of $\epsilon=3.5$ eV or 5.61×10^{-12} erg, and expressing q in coulomb, eq (2) can be written as:

$$I_g=2.48\times10^{-6}A_R(\Delta X/\Delta t)\frac{(\mu_{en}/\mu)}{(\mu_{en}/\rho)_{\text{air}}}\exp(-\mu d_s)\times\left[1-\frac{\exp(-\mu w)}{\mu L_n+1}+\frac{\mu d_s}{1+(s_pd_s)/D_p}\right]\text{ampere.} \tag{2a}$$

For values $\mu L_n << 1$, $\mu w << 1$, and $\mu d_s << 1$, and $s_p = 0$, eq (2a) is reduced to the equation given for I_g in a previous paper (eq (19) in ref. [1]) having been derived under the assumption of negligible attenuation of the radiation in the charge collecting volume.

If the cell surface is covered by a contact or any other layer to ensure electronic equilibrium in the cell surface region, the values of I_g obtained from eqs (2) and (2a) have to be multiplied by an attenuation factor exp $(-\mu_c d_c)$ where μ_c and d_c are the attenuation coefficient and thickness of the surface cover, respectively.

3.2. Discussion of Basic Equations

Equation (3) derived from the basic rectifier theory [13] will not be discussed here, but detailed consideration will be given to eq (2) for the generated photocurrent I_g which is of main interest in this investigation.

For the discussion of eq (2), *effective* diffusion lengths may be defined as:

$$L_n' = L_n \frac{a_n}{\mu^2 L_n^2 - 1}; \qquad L_p' = L_p \frac{a_p}{\mu^2 L_p^2 - 1} \tag{4}$$

which determine the electric charge collected by diffusion of electrons and holes from the base and surface layer into the depletion region. The average diffusion lengths L_n and L_p are material constants, but L_n' and L_p' are functions of the same parameters as a_n and a_p.

The dependence of the effective diffusion lengths on these parameters is shown in figures 1 to 3. The effective diffusion lengths are given as dimensionless relative values (L_n'/L_n) and (L_p'/L_p), and were calculated by using eqs (A. 13) given in the appendix. The graphs were calculated for photon energies corresponding to effective energies of heavily filtered x rays investigated as given below (table 1).

With increasing ratios of layer thickness to average diffusion length, the effective diffusion lengths increase and approach saturation values for $d_b/L_n > 1$ and $d_s/L_p > 1$ (figs. 1 and 2). With decreasing photon energy, the effective diffusion lengths of minority carriers in the base layer (L_n'/L_n) decrease but increase for those in the surface layer (L_p'/L_p). This increase, however, is offset by the increased attenuation of the radiation in the surface layer taken into account by the factor exp $(-\mu d_s)$ in eq (2). For both types of minority carrier, the effective diffusion lengths are decreased if surface recombination velocity is increased.

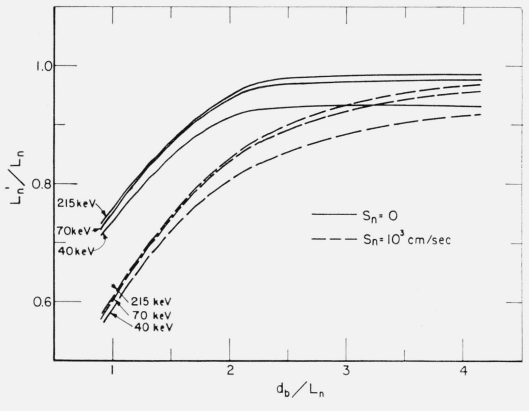

FIGURE. 1. *Relative effective diffusion lengths of electrons in the* p*-type silicon base layer* $[L_n'/L_n = a_n/(\mu^2 L_n^2 - 1)]$ *calculated as function of* d_b/L_n *for different photon energies, assuming different values of* s_n. L_n *assumed* $= 420\ \mu$.

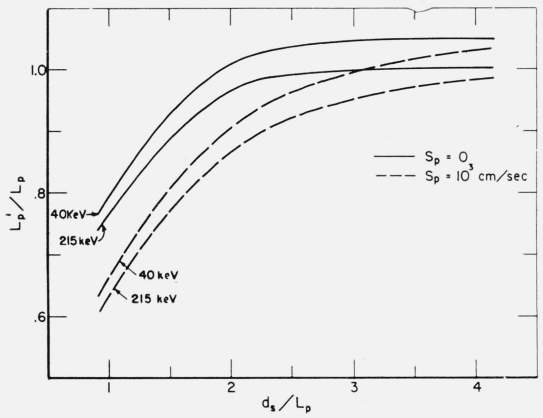

FIGURE 2. *Relative effective diffusion lengths of holes in the* n*-type silicon surface layer* $[L_p'/L_p = a_p/(\mu^2 L_p^2 - 1)]$ *calculated as function of* d_s/L_p *for different photon energies, assuming different values of* s_p. L_p *assumed* $= 100\ \mu$.

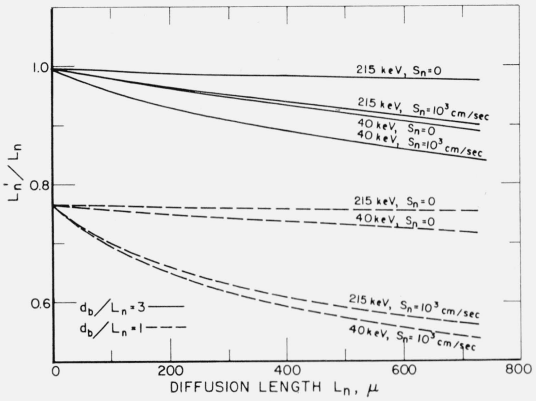

FIGURE 3. *Relative effective diffusion lengths* L_n'/L_n *of electrons in the p-type silicon base layer calculated as function of* L_n *for different photon energies, assuming different values of* d_b/L_n *and* s_n.

The widths of the surface layer and the junction region under the photovoltaic mode of operation may be assumed to be small compared with the diffusion lengths of minority carriers. The generated photocurrent I_g will, therefore, mainly consist of minority carriers produced by the radiation in the base layer. For the cell configuration under consideration, I_g will be determined by the effective diffusion length L_n' of electrons produced in the p-type base.

Assuming a constant value of L_n, L_n' will increase with increasing base layer thickness until a_n reaches a saturation value. A further increase of sensitivity could not be achieved by further increase of the base layer thickness d_b, but only by increasing L_n. The highest sensitivity would be obtained by increasing L_n as much as possible and increase the base layer thickness so that a_n remains at the saturation value. With increasing L_n, the charge collected from the base layer will not increase proportional to L_n, but at a smaller rate, dependent on the photon energy and the amount of surface recombination (fig. 3). With increasing L_n, L_n' will increase at a smaller rate than L_n, i.e., L_n'/L_n will decrease.

Graphs of the energy dependence of the photovoltaic current sensitivity of a p-n junction cell calculated by using eq (2) and assuming different values of L_n, d_b/L_n, and s_n are shown in figures 4 and 5. The photovoltaic current sensitivity is given as the generated photocurrent I_g obtained with an irradiated surface area of 1 cm² at an exposure rate of 1 R/min or $\frac{1}{60}$ R/sec. The calculations were made for monoenergetic x rays, the quality of the radiations being expressed in half-value layers (HVL) of aluminum. Values of μ_{en} and μ for silicon were obtained from data given by White Grodstein [14] and Nelms [15]. Values of $(\mu_{en}/\rho)_{air}$ were taken from ICRU reports [16]. Other parameters used in the calculations, but not shown in

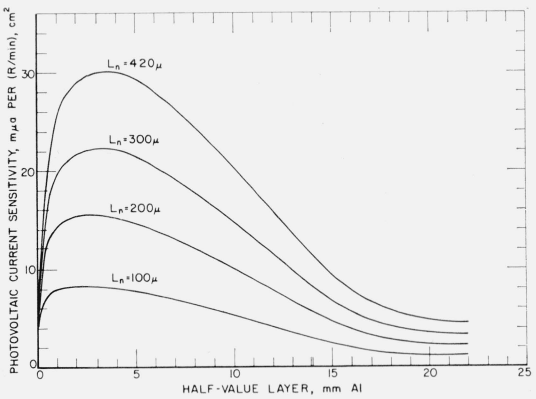

FIGURE 4. *Energy dependence of the short-circuit current obtained at an exposure rate of 1 R/min and 1 cm² irradiated silicon surface, as calculated for different values of* L_n, *assuming* $d_b/L_n >> 1$, $s_n = 0$.

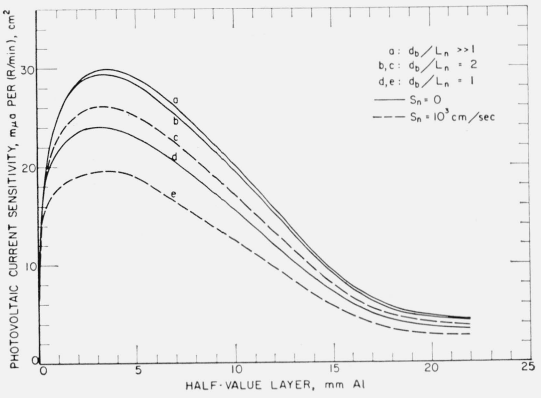

FIGURE 5. *Energy dependence of the short-circuit current obtained at an exposure rate of 1 R/min and 1 cm² irradiated silicon surface as calculated for different values of* d_b/L_n *and* s_n, *assuming* $L_n = 420$ μ.

figures 4 and 5, were: $d_s=2.0\ \mu$, $d_s/L_p<<1$, $s_p=10^3$ cm/sec, $D_p=10$ cm^2/sec, and $D_n=30$ cm^2/sec. Considering the small photovoltages obtained with x rays, the junction width w was assumed to be constant for all calculations. Its value was approximately calculated as $w=7.0\ \mu$ by using the relation

$$w=1/3\sqrt{\rho V_0} \tag{5}$$

assuming the resistivity ρ of the p-type base layer as 1000 Ω-cm and the barrier voltage $V_0=0.5$ volt.

The photovoltaic current sensitivity is strongly dependent on L_n and increases at all energies nearly linearly with increasing L_n (fig. 4). For $L_n=420\ \mu$, the sensitivity reaches a maximum at an HVL of approximately 3.5 mm Al (34.5 keV) which shifts for $L_n=100\ \mu$ to a HVL of 2.5 mm Al (30 keV). However, the ratio between the maximum value of sensitivity to the sensitivity at a HVL of 21.4 mm Al (200 keV) is nearly the same, approximately 6.5, independent of the parameter L_n. The energy dependence is slightly changed, especially at low energies (small HVL) if at constant L_n, the base layer thickness or surface recombination is changed (fig. 5). In accordance with the discussion given above, the sensitivity decreases over the whole energy range when the ratio d_b/L_n is decreased or s_n is increased.

3.3. Circuit Equations

According to eq (2), the generated photocurrent I_g is proportional to the exposure rate, and measurement of the latter should be based on the measurement of I_g or any other quantity linearly related to it.

Equation (3) can be written in current notation as

$$I_j=I_o\,[\exp\,(qV/kT)-1] \tag{6}$$

from which one obtains from eq (1):

$$I=I_g-I_o\,[\exp\,(qV/kT)-1] \tag{7}$$

$$V=\frac{kT}{q}\ln\left[\frac{I_g-I}{I_o}+1\right]. \tag{8}$$

Here, V is the forward voltage at the junction produced by irradiation. If the series cell resistance consisting of the contact and bulk resistances is negligibly small compared with the load resistance R_L, then V is equal to the photovoltage measured between the terminals of the cell

$$V=IR_L. \tag{9}$$

The current I_s measured under short circuit conditions ($R_L=0$, $V=0$) and the voltage V_{oc} measured under open circuit conditions ($R_L=\infty$, $I=0$) are:

$$I_s=I_g \tag{10}$$

$$V_{oc}=\frac{kT}{q}\ln\left(\frac{I_g}{I_o}+1\right). \tag{11}$$

The short circuit current I_s, which is equal to I_g and therefore proportional to the exposure rate, can not actually be measured, but only determined by extrapolation of the measured output current to zero load resistance, while quantities directly measurable as I, V, and V_{oc}, are not linearly related to I_g. However, under certain conditions, proportionality between I and I_g can be sufficiently approached. Introducing the static junction resistance at the forward junction voltage V

$$(R_j)_V=\frac{V}{(I_j)_V},$$

one obtains from eqs (1) and (9)

$$I=I_g-\frac{V}{(R_j)_V}=I_g\left[1+\frac{R_L}{(R_j)_V}\right]^{-1} \tag{12}$$

$$V=(I_j)_V(R_j)_V=(I_g-I)(R_j)_V=IR_L \tag{13}$$

$$V_{oc}=I_g(R_j)_{V_{oc}} \tag{14}$$

The junction resistance is voltage dependent and decreases with increasing forward voltage. Proportionality of the measured values of I and V with I_g or the exposure rate, will be obtained if $(R_j)_V$ is constant or if $R_L/(R_j)_V<<1$.

At small voltages or values of $I_g/I_o<<1$, the junction resistance may be considered as constant, its value being derived from eq (6) as

$$(R_j)_o=\frac{kT}{qI_o}. \tag{15}$$

The resistance $(R_j)_o$, also called the zero voltage junction resistance, is inversely proportional to the reverse saturation current I_o. Thus, at small photovoltages as obtained with small exposure rates, the values of I, V, and V_{oc} may be considered to be proportional to I_g or the exposure rate. For large exposure rates or large I_g, proportionality between I or V and the exposure rate can be retained by reducing the load resistance R_L, thereby reducing the photovoltage and the ratio $R_L/(R_j)_V$. No such regulation is possible for the open-circuit voltage V_{oc} which at larger values follows a logarithmic dependence on exposure rate (eq (8)).

It is known that eq (6) does not satisfactorily describe the voltage dependence of the measured junction current I_j of a silicon diode [17], but may be considered as an approximation applicable to the operation of photovoltaic cells [8]. Measurements reported here were evaluated by considering the junction leakage current I_j obtained from the current-voltage characteristic measured for small forward voltages. Values of short-circuit currents discussed below were determined either by extrapolating the measured photovoltaic output current I to zero load resistance, or by adding to I the junction current I_j, given by the measured current-voltage characteristic of the cell for the respective photovoltage values (eq (1)).

4. Experimental Procedure

The silicon radiation detector cells investigated were commercially available encapsulated cells of the diffused p-n junction type, provided with a thin protective aluminum layer on the surface. According to the manufacturer's specification, the cells were made of 1000 Ω-cm p-type silicon with an n-type layer on the sensitive surface. The diffusion depth was approximately 2 μ and the thickness of the protective aluminum layer approximately 0.5 to 1.0 μ. Cells were exposed to radiation under normal air pressure and were covered with a light-tight paper cover.

The x-ray sources were a 250-kV tube and a 50-kV beryllium-window-type tube with an inherent filtration of approximately 4.0 mm Al and 0.25 mm Be respectively. The x-ray tubes were tungsten target tubes operated by stabilized constant voltage supplies. The different qualities of radiations obtained by using different filtration are shown in table 1. Exposure rates of heavily and moderately filtered x rays were measured by R-meters which had been calibrated for each investigated type of radiation against the NBS standard free-air chamber. Exposure rates of lightly filtered x rays were measured with an NBS free-air chamber.[4]

[4] Exposure rate measurements with the free-air chamber were carried out by Paul Lamperti of the NBS X-Ray Standards Section.

TABLE 1. *Types of radiations investigated*

kvcp	Approx. inherent filter	Added filter	Target distance	Approx. HVL
Lightly filtered x rays				
	(*mm* Be)	(*mm* Al)	(*cm*)	(*mm* Al)
20	0.25	0	60	0.07
20	.25	0.5	60	.25
30	.25	0	60	.09
30	.25	0.5	60	.42
50	.25	0	60	.12
50	.25	0.5	60	.64
50	.25	1.0	60	.93

kvcp	Approx. inherent filter	Added filter		Approx. HVL
		Al	Cu	
Moderately filtered x rays				
	(*mm* Al)	(*mm*)	(*mm*)	(*mm* Al)
60	4.0	0	0	2.79
75	4.0	0	0	3.41
100	4.0	1.0	0	5.05
150	4.0	1.0	0.25	10.1
200	4.0	1.0	0.5	13.2
250	4.0	1.0	1.0	16.2

kvcp	Approx. inherent filter	Added filter			Approx. effective energy	Approx. HVL
		Pb	Sn	Cu		
Heavily filtered x rays						
	(*mm* Al)	(*mm*)	(*mm*)	(*mm*)	(*keV*)	(*mm* Al)
50	4.0	0.12	0	0	40	4.4
100	4.0	0.53	0	0	70	11.2
150	4.0	0	1.5	4.0	120	16.8
200	4.0	0.7	4.0	0.6	170	19.5
250	4.0	2.7	1.0	0.6	215	21.5

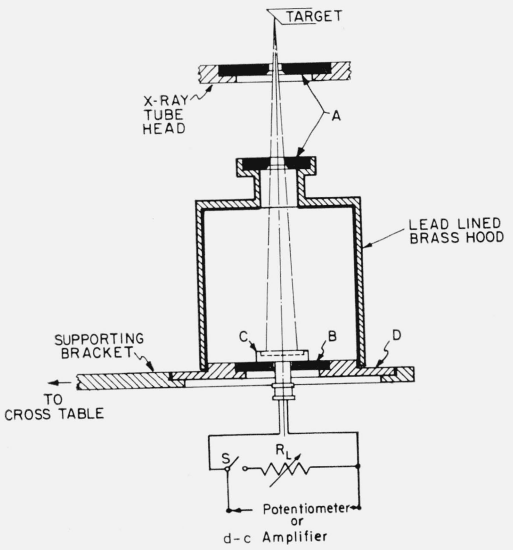

FIGURE 6. *Sketch of mounting of radiation detector cell showing geometry of irradiation.*

(A) Lead diaphragms; (B) Bakelite disk; (C) Silicon radiation detector cell; (D) Lead disk, being removed for measurement of exposure rates in air.

The x-ray beams, if not otherwise stated, were collimated by lead diaphragms mounted in a fixed position relative to the cell. The beam diameter at the cell surface was smaller than the cell area so that no radiation was passing through the cell casing before hitting the sensitive cell surface. The mounting of the cell in the vertical beam of the 250-kV x-ray tube is shown in figure 6. The size and position of the beam spot were checked radiographically. For correct positioning of the cell, the whole fixture was mounted on an adjustable cross-table. For measurements in the horizontal beam of the 50-kV x-ray tube, a holder was used containing the cell and the beam-size defining diaphragm, and mounted on the optical bench used for the low-energy NBS air chamber.

The photovoltaic output current and the open-circuit voltage were measured by a null method with a potentiometer. The photocurrent was determined by measuring the voltage drop over a load resistance of known value.

5. Measurements

5.1. Exposure Rate Dependence

The exposure rate dependence of the photovoltaic output current I and the open circuit voltage V_{oc} measured on two radiation detector cells of different size is shown in figure 7. The cells were fully irradiated with lightly filtered 30-kV x rays of 0.3 mm Al half-value layer (HVL). The different exposure rates were obtained by changing the x-ray tube current. Due to the strong absorption of the low-energy radiation in the cell casing, the sensitive areas of the two cells may be assumed to be approximately equal to their nominal sensitive free surface areas of 5 mm^2 and 2.0 cm^2 respectively.

The photovoltaic current of the 5 mm^2 cell, measured with a load resistance of 10^5 Ω is proportional to exposure rates up to 10^5 R/min, the highest exposure rate investigated. The photocurrent of the larger cell (2.0 cm^2) measured with a smaller load resistance of 10^4 Ω shows a slight deviation from linear response for exposure rates above 2000 R/min. Due to its smaller cell resistance, the condition $R_L/(R_j)_V << 1$ was not fulfilled at the relative high photovoltages, when using a load resistance of 10^4 Ω. By reducing the load resistance, the linear dependence of the photocurrent could be extended to higher exposure rates, approaching the short-circuit dependence ($R_L=0$) on exposure rate shown in figure 7. The ratio of the photocurrents of the two cells is in good agreement with the ratio of their surface areas which is approximately 40:1.

The open circuit voltages show a nearly linear exposure rate dependence at low exposure rates and follow a logarithmic dependence at higher exposure rates (eq (11)). They are of the same order of magnitude for both cells, and differ at exposure rates of 5000 R/min by only about 15 percent. The open circuit voltage V_{oc} is a function of the ratio I_g/I_o, I_g and I_o being proportional to the irradiated and total cell surface respectively. Therefore, for fully

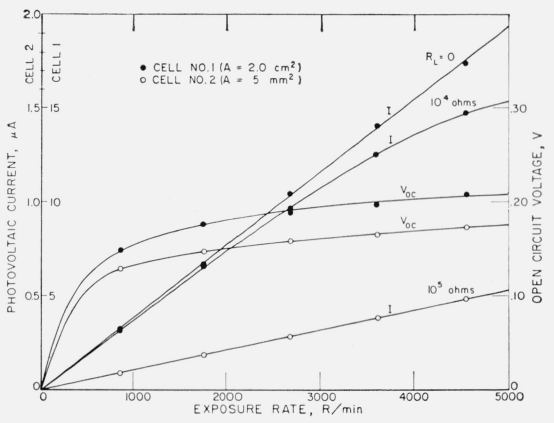

FIGURE 7. *Exposure rate dependence of open-circuit voltage and photovoltaic output current measured with 30-kV lightly filtered x rays of 0.09 mm* Al *HVL.*

irradiated cells of the same type, and the same quality of radiation, V_{oc} should be independent of the cell area. The small difference observed may be explained by some differences in design and structure of the cell.

The response times to irradiation were short, within the response times of the measuring instruments, and no fatigue of the cells was observed during irradiation. At constant temperatures, measurements of the photocurrent were reproducible within one percent. The open-circuit voltage shows a greater noise than the photocurrent and is strongly temperature dependent, making its measurement less accurate.

5.2. Temperature Dependence

For measuring the temperature dependence, the detector cells were placed inside a drying oven and fully irradiated through the oven wall consisting of nonmetallic heat insulating material. The oven temperature was thermostatically controlled within ± 1 °C.

The photovoltaic current-voltage characteristic of a silicon radiation detector cell of 2.0 cm^2 surface area, measured at different temperatures between approximately 25 and 50 °C, is shown in figure 8. These characteristics were measured with 100 kV x rays filtered by 2 mm Al and the oven wall at a constant exposure rate of approximately 50 R/min, and were obtained by changing the load resistance R_L. The intercepts of the load lines with the characteristics give the photocurrent and photovoltage at the respective load resistance and temperature. The short circuit current and the open-circuit voltages at different temperatures are given by the intercepts of the characteristics with the current and voltage axis respectively. With increasing temperature, the open-circuit voltage decreases and the short circuit increases slightly. The load lines through the intersections of these characteristics indicate the load resistances required to keep the temperature dependence in the temperature interval considered at a minimum. According to figure 8, the optimum load resistance for the investigated cell with regard to temperature dependence of photocurrent and photovoltage at the exposure rate under consideration is approximately 10^4 Ω for the temperature interval between 25.6 and 39.2 °C, and about 5×10^3 Ω for temperatures between 39.2 and 49.4 °C.

The relative changes of photocurrent and open-circuit voltage with increasing temperature measured on a cell of 5 mm^2 surface area at the same exposure rate, and using different load resistances, are shown in figure 9. The temperature dependence is qualitatively the same as that shown in figure 8. At 25 °C, the short-circuit current ($R_L=0$) increases by 0.32 percent per °C, and the open-circuit voltage ($R_L=\infty$) decreases by 2.2 percent per °C, with increasing

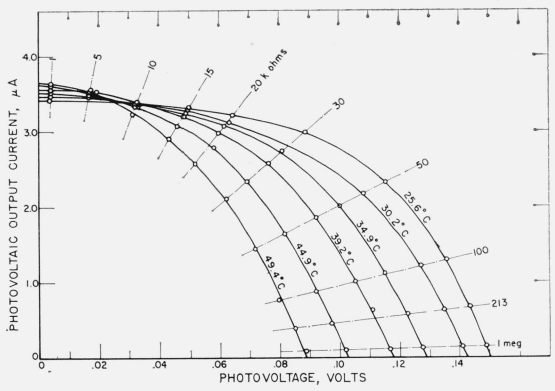

FIGURE 8. *Photovoltaic current-voltage characteristic at different temperatures measured on a silicon radiation detector cell of 2.0 cm² surface area, with indication of load lines for different load resistances.*

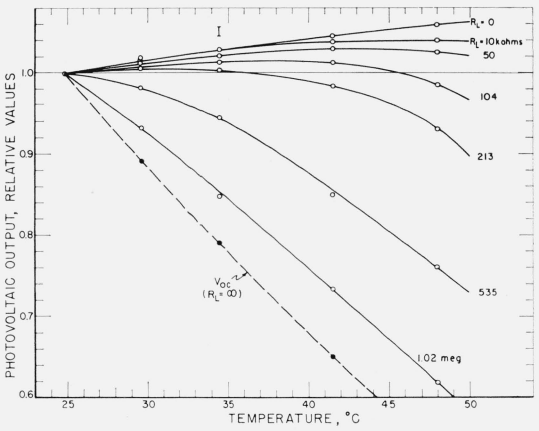

FIGURE 9. *Relative change with temperature of open-circuit voltage and photovoltaic output current measured with different load resistances on a silicon radiation detector cell of 5.0 mm² surface area.*

temperature. For finite load resistances, the temperature dependence of the photocurrent lies between these two extreme values. Due to the larger junction resistance of this cell compared with the cell of 2.0 cm^2 surface, the optimum load resistances are of higher values for the smaller cell. For instance, with $R_L = 1.04 \times 10^5$ Ω, the photocurrent changes between 25 and 45 °C by less than one percent.

The temperature dependence of the photovoltaic response is mainly due to the temperature dependence of I_j. In general, in order to keep the temperature dependence low, the value of the load resistance should be chosen of such a value that the condition $R_L/(R_j)_V << 1$ remains satisfied over the temperature and photovoltage range under investigation.

No definite explanation can be given for the increase of the short-circuit current with increasing temperature. A similar temperature dependence of the short-circuit current produced by visible light, was explained by the displacement of the absorption spectrum of silicon due to a change of the band gap energy [18]. This explanation can apparently not be applied to the short-circuit current produced by x rays. The temperature dependence of the amount of x-ray energy absorbed per unit volume of silicon may be assumed to be negligible. There may exist a temperature dependence of the average energy ϵ of electron-hole pair production, but the change of band gap energy with change in temperature should be of little influence. The band gap energy accounts for approximately only a third of the value of ϵ [12], and decreases only by approximately 0.04 percent per °C with increasing temperature [19]. Another explanation could be the decrease of the series cell resistance (bulk and contact resistance), with increasing temperature. As estimated from the forward characteristic of the cell investigated, the cell series resistance was approximately 0.01 percent of the zero voltage junction resistance and could therefore have only a negligible influence on the measured temperature dependence of the short-circuit current. Another explanation would be to assume an increase of the diffusion lengths of minority carriers due to the temperature dependent changes of recombination and trapping rates [20].

5.3. Energy Dependence

The energy dependence of the photovoltaic response was measured for heavily, moderately, and lightly filtered x rays (table 1). The photocurrent was determined by measuring the voltage drop over the input resistance of an amplifying d-c microvolt-ammeter serving as load resistance in the cell circuit. The input resistance was variable corresponding to the different measuring ranges of the instrument, so that the input resistance could be chosen small enough to keep the temperature dependence of the photocurrent at a low level. The voltage-amplifying gain at all energies used was 1000, and the amplified voltage drop was measured with a potentiometer with a precision of a few tenths of a percent. The exposure rates were approximately 0.5 to 1.0 R/min for heavily filtered x rays and approximately 5.0 to 50.0 R/min for moderately and lightly filtered radiations. The x-ray beam was collimated as described above.

The charge collecting volume in the radiation detector cell extends from the inside of the silicon up to the irradiated surface. Due to the lack of compensation of charge carried away by high-energy electrons produced in the surface region, the ionization near the surface is only gradually increasing with increasing depth in the silicon until a maximum value is reached at a depth approximately equal to the maximum range of the radiation-produced high-energy electrons. In order to compensate this ionization deficiency and approach electron equilibrium conditions in the surface region, the cell surface was covered with thin layers of aluminum which has an atomic number ($Z_{Al} = 13$) close to that of silicon ($Z_{Si} = 14$). The photocurrent measured with the cell surface covered with aluminum layers of different thicknesses is shown in figure 10. Covering the silicon surface with aluminum is equivalent to moving the charge-collecting volume deeper into the silicon. The photocurrent shows, therefore, first an increase with increasing layer thickness reaching a broad maximum at a layer thickness equal to the maximum electron range R in aluminum which may be assumed to be approximately the same as in silicon. A further increase of layer thickness reduces the photocurrent due to the attenuation

of the radiation in the aluminum layer which again may be assumed to be approximately equal to that of a silicon layer of the same thickness. The higher the photon energy, the greater the rate of the initial increase of the photocurrent. However, even for 250-kV, heavily filtered x rays ($h\nu_{eff}$=215 keV), the maximum photocurrent was found to be only by a few percent larger than that measured without additional surface layer. Slightly different values, but of the same order of magnitude, were measured with different individual cells of the same type. This indicates that the ionization deficiency in the surface region may be assumed to be small compared with the total charge collected.

The following measurements of the energy dependence of the photovoltaic current were all carried out with the cell surface covered by an aluminum layer 325 μ thick, equal to the electronic equilibrium thickness for the highest photon energy (250 keV) considered here (fig. 10).

The energy dependence of the photovoltaic current sensitivity of a diffused silicon p-n junction cell as measured for different qualities of radiation is shown in figures 11, 12, and 13. The sensitivity is expressed by the short-circuit current measured at an exposure rate of 1 R/min and an irradiated cell surface of 1 cm^2. The values of the short-circuit current, assumed to be equal to I_g, were derived from the output current I, measured at a finite load resistance, using eq (12). All values were corrected for a cell temperature of 22 °C considering the measured temperature dependence of the cell leakage-current and short-circuit current.

Relative values of the photovoltaic current sensitivity for heavily filtered x rays are shown in figure 11 as a function of effective photon energy. The measured currents were corrected for attenuation in the aluminum surface layer, which is very small for these types of radiations. The values of sensitivity are normalized to unity for 250-kV x rays ($h\nu_{eff}$=215 keV), the normalized value having been measured as

$$I_s=4.45\times10^{-9}\text{ A (R/min)}^{-1}\text{cm}^{-2}.$$

For a comparison of measured and theoretical values, the photovoltaic current sensitivity was calculated according to eq (2a), assuming monoenergetic radiations. All cell parameters except L_n were assumed to be the same as chosen for the calculation of the energy dependence of the current sensitivity shown in figure 4. The value of the diffusion length L_n was determined by solving eq (2a), with I_g given by the short-circuit current measured at 1 R/min and 1 cm^2 irradiated cell area, and corrected for attenuation in the aluminum layer. The width d_b of the base layer, assumed to be approximately equal to the total thickness of the silicon wafer, was determined by x-ray radiography [5] as d_b=1.4 mm. It was therefore assumed that condition $d_b/L_n >> 1$ was fulfilled and the use of the simplified eq (2a) justified.

Values of L_n calculated in this way from currents measured at different effective energies were not of a constant value, but were slightly increasing with decreasing energy, the value derived from measurements with 250-kV x rays being L_n=420 μ.[6] When using this value of L_n for the calculation of the sensitivity at different photon energies, the relative measured values are consequently higher than the calculated ones shown as relative values in figure 11. The ratio of measured to calculated sensitivity reaches a maximum of approximately 1.3 between 70 and 100 keV.

The apparent energy dependence of L_n, which should be a constant, shows that an energy dependent factor would have to be included in eqs (2) and (2a), in order to bring measured and calculated sensivity values into agreement. A similar energy dependence of the ratio of measured and calculated sensitivities was observed in a previous investigation of silicon solar cells [1], and was there tentatively explained by a reabsorption of scattered Compton photons.

The photovoltaic current sensitivity measured with moderately and lightly filtered x rays of half-value layers between 0.07 mm Al and 16.0 mm Al is shown in figure 12 (curve b). The

[5] The x-ray photographs of the detector cells were made by L.A. Dobak of the NBS Dosimetry Section.

[6] This value of L_n is in good agreement with that determined by Pfister [21] in a similar way, using monochromatic (characteristic) x rays.

sensitivity reaches a maximum at a HVL of approximately 4.0 mm Al which is only three times larger than its value at 16.0 mm Al HVL. The strong decrease at smaller HVL is partly due to the attentuation of the radiation in the added aluminum layer. Curve a in figure 12 shows the sensitivity obtained by relating the measured photocurrent to the radiation incident on the silicon surface after having passed the aluminum cover layer. The attenuation of the radiation and change of its quality (expressed by the HVL) due to the absorption in the aluminum layer, were obtained from experimentally measured attenuation curves of aluminum, so far as they were available for the types of radiation investigated. The maximum of the attentuation-corrected sensivity is shifted to a HVL of 3.5 mm Al and is approximately 9 percent higher than the maximum sensitivity measured with the aluminum cover.

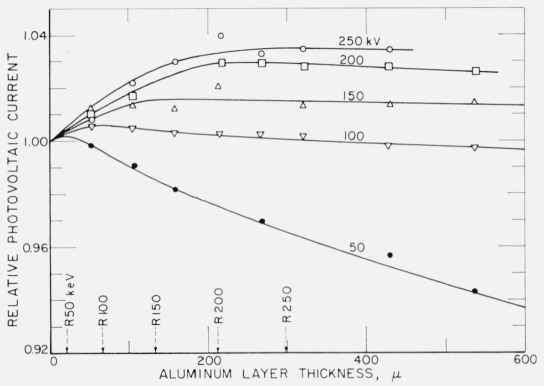

FIGURE 10. *Relative change of photovoltaic output current with increasing thickness of aluminum layer laid on silicon surface as measured with heavily filtered x rays obtained at operating voltages as shown.*

Indicated values of maximum ranges R of electrons in aluminum corresponding to maximum photon energies of radiations investigated agree with layer thicknesses at maximum current values.

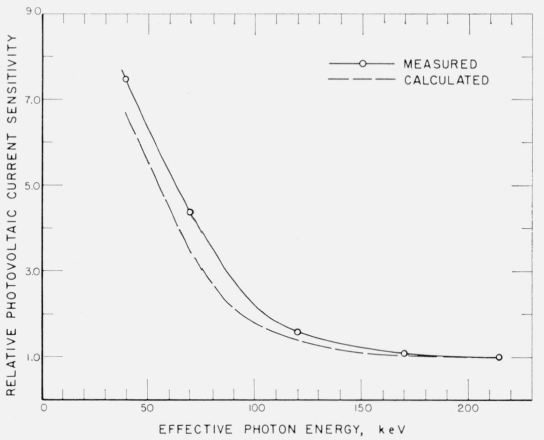

FIGURE 11. *Energy dependence of short-circuit current per R/min and cm² irradiated silicon surface given in relative values as measured with heavily filtered x rays (see table 1) and as calculated for monoenergetic radiations, assuming* $L_n = 420\ \mu$.

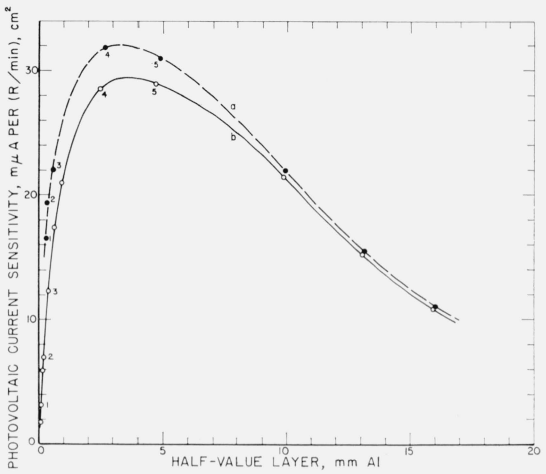

FIGURE 12. *Energy dependence of short-circuit current per R/min and cm² irradiated silicon surface measured with moderately and lightly filtered x rays (see table 1):*

○, as measured with the silicon surface covered with a 325-μ-thick aluminum layer; ●, corrected for attenuation and change of quality of radiation in the aluminum surface layer. Numbers shown near points indicate corresponding measured and corrected values.

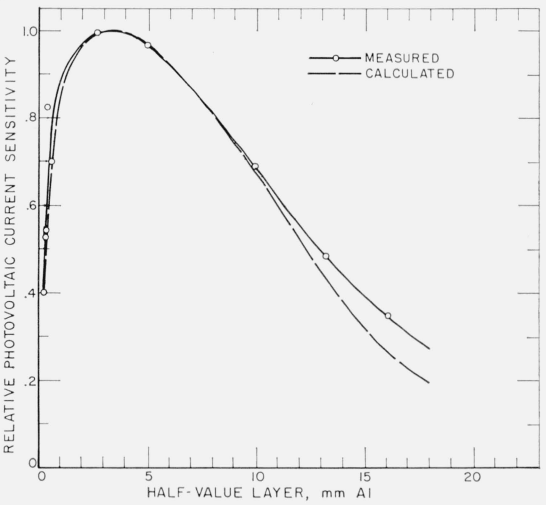

FIGURE 13. *Energy dependence of short-circuit current per R/min and cm² irradiated silicon surface given in relative values as measured with moderately and lightly filtered x rays (see table 1) and as calculated for monoenergetic radiations, assuming* $L_n = 420\ \mu$.

Measured values shown were corrected for attenuation in the aluminum surface layer.

A good qualitative agreement is obtained when comparing sensitivities measured with moderately and lightly filtered x rays and values calculated for monoenergetic radiations. Measured sensitivities corrected for attenuation in the aluminum surface layer, and values calculated assuming a constant L_n=420 μ are shown in figure 13. These sensitivities are given as relative values, normalized to unity at their peak values which are 3.2×10^{-8} A and 3.0×10^{-8} A per R/min and cm^2 irradiated surface for the measured (fig. 12) and calculated sensitivity (fig. 4) respectively. The greater discrepancies between measured and calculated sensitivities at larger HVL are apparently due to the low energy components of the broad spectrum of radiations obtained with moderate and light filtration.

Taking into account that several simplifying assumptions were made in the derivation of eqs (2) and (2a), the energy dependence of the short-circuit current calculated for monoenergetic x rays, and the energy dependence measured with nonmonochromatic radiations may be considered to be in satisfactory qualitative agreement.

6. Conclusions and Summary

A relation has been derived for the photocurrent produced by x rays in silicon radiation detector cells of the *p-n* junction type, giving its dependence on exposure rate, quality of radiation, and electrical and geometrical parameters of the silicon crystal. This relation should be useful for designing a dosimeter using a silicon cell of predetermined performance characteristic.

Silicon radiations detector cells of the diffused *p-n* junction type show a quick and stable response to x rays like silicon solar cells, but have a larger sensitivity. The short-circuit current I_s per cm^2 irradiated cell surface, and the open-circuit voltage V_{oc} extrapolated for a fully irradiated surface produced by heavily filtered 100-kV x rays at an exposure rate of 1 R/min were measured at a cell temperature of 22 °C as follows:

	I_s	V_{oc}
Silicon solar cell:	2.96×10^{-9} A/cm^2,	4.12×10^{-5} V
Silicon radiation detector cell: (covered with a 325-μ-thick aluminum layer)	1.92×10^{-8} A/cm^2,	2.91×10^{-2} V

The short-circuit current I_s is proportional to the irradiated surface area and exposure rate. However, the open-circuit voltage V_{oc}, which is independent of the cell area in the case of a fully irradiated surface, shows a nonlinear dependence on exposure rates in radiation detector cells, even at rather low values of the order of a few R/min. According to eqs (14) and (15), the value of V_{oc} may be approximated by a linear function of I_g, if $I_g/I_o \ll 1$. The saturation current I_o in radiation detector cells is much smaller than in solar cells. Thus, due to the larger value of the ratio I_g/I_o, a nonlinear dependence of V_{oc} will become apparent in radiation detector cells at much smaller exposure rates than in solar cells. For this reason, and because of the large temperature dependence of V_{oc}, measurements of the exposure rates should be based rather on the measurement of the photocurrent I obtained with a suitable load resistance than on the measurement of V_{oc}, except in the case of very small exposure rates.

The measurement of the photovoltaic current can be carried out with high precision, especially when using d-c amplification. The standard deviation of 10 measurements, each being the average of a set of five readings, carried out with heavily filtered 100-kV x rays at an exposure rate of 1 R/min on different days, and at temperatures varying between 20 and 23 °C, was 0.96 percent. The standard deviations for each set of readings made at constant temperature were between 0.1 and 0.3 percent.

The larger current sensitivity of radiation detector cells is apparently due to the larger diffusion length of minority carriers in the high-resistivity base layers of such cells. The high values of V_{oc} observed in radiation detector cells, being several hundred times larger than in solar cells, can be explained by the increased photocurrent and their much larger zero voltage

leakage resistance. This large leakage resistance makes it also possible to use larger load resistances than with solar cells, thereby producing larger photovoltages, without producing a great change in the temperature dependence of the photocurrent. This is especially important for the measurement of small photosignals requiring sensitive instruments of high impedance.

Proportionality between photocurrent and exposure rate was obtained with radiation detector cells up to the highest level investigated of approximately 5000 R/min. The lower limit of the range of measurement of exposure rates was not established, but may be assumed to be dependent on the inherent noise of the photocurrent or photovoltage, and of the noise level of instrumentation used. Under conditions for which temperature dependence of the photocurrent is of less importance, large load resistances could be used, thereby obtaining photovoltages approaching open-circuit voltage values. At an exposure dose of 1 R/min, the open-circuit voltage is, as shown above, of the order of several millivolts. With a noise level of the photosignal of a few microvolts, it should be possible to measure exposure rates of 1 R/hr with sufficient accuracy.

The energy dependence of the short-circuit current measured over a wide range of photon energies, is in good qualitative agreement with calculated values. In particular, the energy dependence measured with heavily filtered x rays of effective photon energies between 40 and 215 keV is similar to that measured on silicon solar cells in this energy range [1]. The photocurrent reaches a maximum value for x rays of low HVL, approximately at 3.5 mm Al for the cells investigated. Around this maximum, the energy dependence is rather small. The value of the photocurrent spreads by only about 10 percent when the HVL of the radiation is changed from 2 mm Al to 7 mm Al. It has been shown by theoretical considerations, that the shape of the energy dependence curve can be changed by changing electrical and geometrical cell parameters determining the photovoltaic current sensitivity of the cell.

It may be concluded from this investigation that the use of silicon radiation detector cells of the *p-n* junction type for x-ray exposure rate measurements is preferable to that of silicon solar cells when operated as photovoltaic cells. A further improvement in sensitivity and performance characteristic of such cells could be achieved by designing silicon cells specially suited for x-ray measurement. The width of the *n*-type surface layer in such cells should be increased, thereby increasing sensitivity, and shape and encapsulation should be of such design that the energy dependence should be reduced, and directional dependence and radiation scattering inside the cell be kept at a minimum.

7. Appendix

The total nonequilibrium current passing through the *p-n* junction under the photovoltaic mode of operation consists, as indicated in figure 14, of: (a) The drift current $(I_g)_{Dr}$ due to

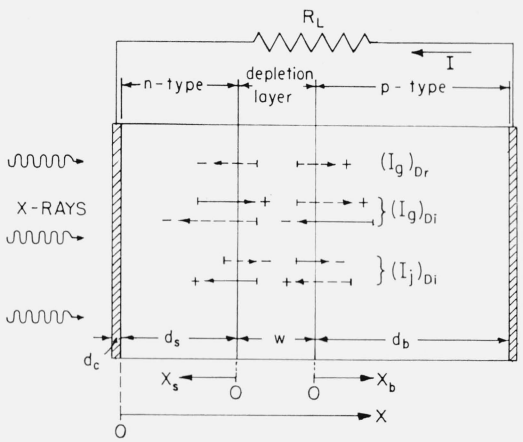

FIGURE 14. *Drift and diffusion currents of electrons and holes in a* p-n *junction cell when operated as a photovoltaic cell.*

Currents of carriers entering or leaving the depletion layer as minority carriers are shown in solid lines.

the electron-hole pairs produced by the radiation in the depletion region and separated by the electric junction field. (b) The diffusion current $(I_g)_{Di}$ of minority charge carriers produced by the radiation in the n-type and p-type layers of the silicon wafer reaching the depletion region by diffusion. Both $(I_g)_{Dr}$ and $(I_g)_{Di}$ are flowing in the reverse current direction of the cell, forming together the generated photocurrent I_g. (c) The diffusion current $(I_j)_{Di}$ in the forward current direction due to the photovoltage V produced by irradiation if the load resistance $R_L > 0$.

The photovoltaic output current I is obtained by adding the different currents passing through a certain section of the circuit which is conveniently chosen at one of the junction edges. If it is assumed that thermal generation and recombination of carriers inside the depletion region can be neglected, then all carriers entering the junction on one side will leave it on the other side without change in carrier density. Electron and hole currents at both junction edges will be the same, making it possible to sum up current components calculated at different sides of the junction.

Calculating the drift current $(I_g)_{Dr}$ and the net diffusion current

$$I_{Di} = (I_g)_{Di} - (I_j)_{Di}$$

separately, one obtains the photovoltaic output current

$$I = (I_g)_{Dr} + I_{Di}. \tag{A.1}$$

In the following calculation the radiation is assumed to be monoenergetic and incident on the n-type surface layer of the cell in the positive x-direction perpendicular to the junction (fig. 14).

(a) *Drift current density.* The generation rate of charge carriers produced by the radiation at a distance x inside the silicon wafer is

$$g(x) = g_s \exp(-\mu x) \tag{A.2}$$

if g_s is the carrier generation rate at the silicon surface which is the number of electron-hole pairs produced per cubic centimeter per second in a thin layer of thickness dx at the irradiated silicon surface.

Assuming total charge collection of charge carriers produced by the radiation inside the junction region, one obtains

$$(J_g)_{Dr} = q \int_{x=d_s}^{x=(d_s+w)} g(x)dx = [(qg_s/\mu) \exp(-\mu d_s)][1 - \exp(-\mu w)] \tag{A.3}$$

The drift current is flowing in the positive x-direction, which is, as assumed, in the reverse current direction of the cell.

(b) *Diffusion current density.* Assuming that there is no charge carrier recombination in the junction region, the total diffusion current is calculated as the sum of diffusion currents of holes and electrons entering or leaving the junction region as minority carriers.

$$J_{Di} = J(p)_{Di} + J(n)_{Di} \tag{A.4}$$

or

$$J_{Di} = -qD_p \left(\frac{dp}{dx}\right)_{x=ds} + qD_n \left(\frac{dn}{dx}\right)_{x=(d_s+w)}. \tag{A.5}$$

Introducing new variables (fig. 14)

$$x_s = d_s - x \text{ and } x_b = x - (d_s + w), \tag{A.6}$$

one obtains

$$J_{Di} = qD_p \left(\frac{dp}{dx_s}\right)_{x_s=0} + qD_n \left(\frac{dn}{dx_b}\right)_{x_b=0}. \tag{A.6a}$$

The values of $\left(\frac{dp}{dx_s}\right)$ and $\left(\frac{dn}{dx_b}\right)$ are obtained by solving the continuity equations for electrons and holes under steady-state conditions.

n-region:

$$D_p \frac{d^2p}{dx_s^2} - \frac{p-p_n}{\tau_p} + g(x_s) = 0 \tag{A.7}$$

p-region:

$$D_n \frac{d^2n}{dx_b^2} - \frac{n-n_p}{\tau_n} + g(x_b) = 0 \tag{A.7a}$$

where

$$g(x_s) = g(x_s)_o \exp(\mu x_s) \tag{A.8}$$

$$g(x_b) = g(x_b)_o \exp(-\mu x_b) \tag{A.8a}$$

if $g(x_s)_o$ is $g(x_s)$ at $x_s=0$, and $g(x_b)_o$ is $g(x_b)$ at $x_b=0$.

The following boundary conditions were used for solving the continuity eqs (A.7 and A.7a), assuming surface carrier-recombination on the surface and base contact of the silicon wafer:

n-side:

$$x_s=0;\ p=p_n \exp(qV/kT) \tag{A.9}$$

$$x_s=d_s;\ \frac{dp}{dx_s} = -\frac{s_p}{D_p}(p-p_n).$$

p-side:

$$x_b=0;\ n=n_p \exp(qV/kT) \tag{A.10}$$

$$x_b=d_b;\ \frac{dn}{dx_b} = -\frac{s_n}{D_n}(n-n_p).$$

Using the relations

$$L_n=\sqrt{D_n\tau_n};\ L_p=\sqrt{D_p\tau_p} \tag{A.11}$$

one obtains as a result of the calculation for the diffusion currents:

$$J(p)_{Di} = g(x_s)_o \frac{qL_p}{\mu^2 L_p^2 - 1} a_p - \frac{qp_nD_p}{L_p} b_p [\exp(qV/kT) - 1] \tag{A.12}$$

$$J(n)_{Di} = g(x_b)_o \frac{qL_n}{\mu^2 L_n^2 - 1} a_n - \frac{qn_pD_n}{L_n} b_n [\exp(qV/kT) - 1] \tag{A.12a}$$

The factors a_p, a_n, b_p, and b_n are given by the following equations where $S_p=(s_pL_p)/D_p$, and $S_n=(s_nL_n)/D_n$:

$$a_p = \frac{(\mu L_p + S_p)\exp(\mu d_s) - \sinh(d_s/L_p) - S_p\cosh(d_s/L_p)}{\cosh(d_s/L_p) + S_p\sinh(d_s/L_p)} - \mu L_p$$

$$a_n = \mu L_n - \frac{(\mu L_n - S_n)\exp(-\mu d_b) + \sinh(d_b/L_n) + S_n\cosh(d_b/L_n)}{\cosh(d_b/L_n) + S_n\sinh(d_b/L_n)} \tag{A.13}$$

$$b_p = \frac{\sinh(d_s/L_p) + S_p\cosh(d_s/L_p)}{\cosh(d_s/L_p) + S_p\sinh(d_s/L_p)}$$

$$b_n = \frac{\sinh(d_b/L_n) + S_n\cosh(d_b/L_n)}{\cosh(d_b/L_n) + S_n\sinh(d_b/L_n)}.$$

Using eq (A.2) one can substitute in eqs (A.12) and (A.12a):

$$g(x_s)_o = g_s \exp(-\mu d_s) \tag{A.14}$$

$$g(x_b)_o = g_s \exp[-\mu(d_s+w)]. \tag{A.14a}$$

For x rays of the intensity I_R

$$g_s = \frac{I_R \mu_{en}}{\epsilon} \tag{A.15}$$

or assuming the energy required to produce an ion pair in air as $W=33.7$ eV [16] one obtains

$$g_s = \frac{86.9\mu_{en}}{\epsilon(\mu_{en}/\rho)_{\text{air}}} (\Delta X/\Delta t) \tag{A.16}$$

if ϵ is given in erg and $\Delta X/\Delta t$ in R/sec.

The total output current is obtained as the sum of the drift and diffusion currents as given by eqs (A.3) and (A.12). Summing up the radiation dependent parts separately, the photocurrent I is obtained as

$$I = J_g A_R - J_j A_c = I_g - I_j \tag{A.17}$$

if A_R is the irradiated and A_c the total cell surface area and

$$J_g = (86.9q/\epsilon)(\Delta X/\Delta t)\frac{(\mu_{en}/\mu)}{(\mu_{en}/\rho)_{\text{air}}} \exp(-\mu d_s) \times \left\{ [1-\exp(-\mu w)] + \frac{\mu L_p}{\mu^2 L_p^2 - 1} a_p + \frac{\mu L_n \exp(-\mu w)}{\mu^2 L_n^2 - 1} a_n \right\} \tag{A.18}$$

$$J_j = q[\exp(qV/kT) - 1]\left(\frac{p_n D_p}{L_p} b_p + \frac{n_p D_n}{L_n} b_n\right). \tag{A.19}$$

The terms in the braces of eq (A.18) indicate the separate current contributions by carriers produced in the junction region, and in the surface and base layer of the silicon wafer respectively.

Equations (A.13) for a_p, a_n, b_p, and b_n can be simplified by using approximations applicable under certain conditions:

(1) Surface layer: $d_s << L_p$; $\mu d_s << 1$; $\sinh(d_s/L_p) \sim \frac{d_s}{L_p}$; $\cosh\frac{d_s}{L_p} \sim 1$

$$a_p = \frac{d_s}{L_p}\left[\frac{\mu^2 L_p^2 - 1}{1+(s_p d_s/D_p)}\right] \tag{A.20}$$

$$b_p = \frac{(d_s/L_p)+S_p}{1+S_p(d_s/L_p)}.$$

(2) Base layer: $d_b >> L_n$; $\sinh(d_b/L_n) \sim \cosh(d_b/L_n)$

$$a_n = (\mu L_n - 1)\left[1 - \frac{(\mu L_n - S_n)\exp(-\mu d_b)}{(\mu L_n - 1)(1+S_n)\cosh(d_b/L_n)}\right] \tag{A.21}$$

$$b_n = 1.$$

For small values of S_n or $S_n = 0$, a condition applicable for an ohmic contact, one can assume

$$a_n = \mu L_n - 1. \tag{A.21a}$$

8. References

[1] K. Scharf, Bull. Am. Phys. Soc. (Series 2) **3,** No. 4, 261 (1958); J. Res. NBS **64A,** 297 (1960).
[2] J. W. Moody, G. L. Kendall, and R. K. Willardson, Nucleonics **16,** No. 10, 101 (1958).
[3] J. Calkins, Nucleonics **20,** No. 1, 70 (1962).
[4] W. Rosenzweig, Rev. Sci. Instr. **33,** 379 (1962).
[5] R. L. Cummerow, Phys. Rev. **95,** 16 (1954).
[6] R. Wiesner, Halbleiterprobleme (ed. W. Schottky) **3,** 59 (1956).
[7] G. L. Bir and G. E. Pikus, Soviet Phys.-Tech. Phys. **2,** 419 (1957).
[8] M. Wolf, Proc. IRE **48,** 1246 (1960).
[9] J. J. Loferski and J. J. Wysocki, RCA Review **22,** 38 (1961).
[10] W. W. Gärtner, Phys. Rev. **116,** 84 (1959).
[11] A. J. Tuzzolino, E. L. Hubbard, M. A. Perkins, and C.Y. Fan, J. Appl. Phys. **33,** 148 (1962).
[12] W. Shockley, Solid State Electr. **2,** 35 (1961).
[13] W. Shockley, Bell Syst. Tech. J. **28,** 435 (1949).
[14] G. White Grodstein, NBS Circ. 583 (1957).
[15] A. T. Nelms, NBS Circ. 542 (1953).
[16] Physical Aspects of Irradiation, Recommendations of the International Commission on Radiological Units and Measurements, NBS Handb. 85 (1964).
[17] C. Sah, R. N. Noyce, and W. Shockley, Proc. IRE **45,** 1228 (1957).
[18] M. B. Prince and M. Wolf, J. Brit. Radio Engrs. **18,** 583 (1958).
[19] F. J. Morin and J. P. Maita, Phys. Rev. **96,** 28 (1954).
[20] M. Lax, Phys. Rev. **119,** 1502 (1960).
[21] H. Pfister, Z. angew. Phys. **15,** 407 (1963).

(Paper 68A6–318)